JOURNAL OF MATERIALS SCIENCE 29 (1994) 5399–5406

Non-linear creep behaviour of PET

L. LADOUCE, J. PEREZ, R. VASSOILLE, G. VIGIER
GEMPPM (UA CNRS 341), INSA Lyon, 69621 Villeurbanne cedex, France

The non-linear creep behaviour has been studied on PET films at room temperature. A particular value of the stress, σ_c, was used to characterize the change between the linear to the non-linear domain. The variations of the elastic modulus, the relaxed modulus and σ_c revealed great sensitivity to the morphology of the crystallization. A molecular model of non elastic deformation, assuming (i) hierarchical correlated molecular motion, and (ii) nucleation and expansion of sheared-microdomains, was used to analyse the role of stress on anelasticity. To take into account the two-phase structure of semicrystalline films, a phenomenological series/parallel model was applied to express the mechanical coupling between amorphous and crystalline phases. Quantitative agreement was found between theoretical predictions and experimental data for low and high stresses. However, there was a discrepancy in the rate of recovery because the model predicts a strain recovery slower than the experimental behaviour. Consequently, it is proposed to develop further the molecular model mentioned above by specifying the energy profile of a sheared-microdomain and its stress dependence. Then, the difference between creep and recovery strain rate could be explained.

Nomenclature

A	Anelastic equilibrium compliance
A'	Parameter proportional to the relaxation strength
b	Shear vector
χ	Correlation parameter
χ_i	Particular value in the distribution
χ_e	Average value in the material ($\chi = 0.27$)
χ'	Correlation parameter characterizing the ability of chain orientation
d_a	Amorphous density
d_c	Crystalline density
ϕ	Parameter of the mechanical mixing law
E	Tensile modulus
E_c	Crystalline Young's modulus
g_i	Statistical weight in the distribution
G_0	Shear modulus at 0 K
J_{max}	Creep compliance at the end of the creep time
$J_{max}(0)$	Value of J_{max} for low stresses
J_u	Unrelaxed compliance
$J_i(\chi_i; A_i)$	Calculated compliance for a couple $(\chi_i; A_i)$
J_{exp}	Experimental creep compliance
J_a	Compliance of the amorphous part
J_c	Compliance of the crystalline part
J_{sc}	Compliance of the semi-crystalline material
k	Boltzmann's constant
λ	Parameter of the mechanical coupling law
R	Radius of a shear micro domain
σ_0	Stress necessary to cross the energy barrier only by mechanical activation
T_c	Crystallization temperature
t_c	Creep time
τ_{mol}	Time for a translational motion of a structural unit over a distance comparable to its size
τ_{mol_i}	Particular value of τ_{mol} in the time distribution
τ_β	Characteristic time for the secondary relaxation
τ_0	Time proportional to the Debye time
t_0	Scaling time parameter determined by the experimental value of τ_{mol}
U_β	Activation energy for an elementary molecular motion
X_c	Crystallinity ratio
V_a	Volume fraction of the amorphous part
V_c	Volume fraction of the crystalline part

1. Introduction

Poly(ethylene terephthalate) (PET), the condensation product of terephthalic acid and ethylene glycol, has many important commercial applications, for instance, in the packaging, sports or textile industries. This polymer crystallizes easily with suitable thermal treatments. The mechanism of crystallization of PET from the glassy state has been investigated previously by several authors [1–3]. When this polymer is crystallized, it can be looked upon as a two-phase material exhibiting an amorphous and a crystalline phase [4]. The study of its mechanical properties requires a very good knowledge of the mechanical behaviour of each phase as well as their geometrical distributions which determines their mechanical coupling.

For that purpose, creep experimentation seems to be one of the most useful techniques to study the anelastic and viscoplastic behaviour. Creep tests were

0022–2461

made with the amorphous and partially crystallized PET films presenting different crystallinity ratios. The aim of this work was initially to study the non-linear creep behaviour of PET films. Then, the mechanical response of the amorphous part was analysed using the molecular model of the non-elastic deformation developed in our laboratory [5], which relies on the thermomechanical nucleation of defects and on hierarchical constrained molecular motions. A mixing law based on a phenomenological basis was used to express the mechanical coupling effects between both amorphous and crystalline phases. Finally, this approach allowed a comparison between the mechanical response of the bulk amorphous and that of the amorphous part of semicrystalline films.

2. Experimental procedure

Glassy films of PET have been produced by Rhône Poulenc Films Corporation. The thickness was about 870 μm and the average molecular weight 20 000 g mol^{-1}. The samples were cut from a roll, annealed for 20 min at 363 K (10 K above the glass transition temperature) and then cooled to room temperature. Different crystallinities were obtained by isothermal crystallization at 12 different temperatures, T_c, chosen between 363 and 503 K, in an uncontrolled atmosphere. We verified that no thermal degradation occurred during the annealing by comparing the mechanical properties of two samples crystallized at 453 K. The first one was annealed in a helium atmosphere, the other simply annealed in air. They both had the same crystallinity ratio and the same creep behaviour. The ratio of the crystallization of PET at different temperatures has been investigated on the same films by Benatmane [6]. His results showed that a few minutes were necessary to obtain the equilibrium crystallization for temperatures higher than 393 K and a few hours for lower temperatures. Therefore, a duration of 1 h was chosen for nearly all the temperatures used here. In order to obtain intermediate crystallinities, an annealing time between 2 and 4 h was used for the lowest temperatures. All the specimens were cooled from T_c to room temperature at a cooling rate of 10 K min^{-1}.

The crystallinity ratio was determined with a gradient density column full of carbontetrachloride and ethanol at 296 K with a density of the crystalline phase $d_c = 1.455$ g cm^{-3} and of the amorphous phase $d_a = 1.335$ g cm^{-3}.

Creep tests were performed on an Adamel-Lhomargy MF-11 apparatus [7]. All the displacements were less than 1 mm. The strain was measured by two capacitive sensors with an accuracy of 1 μm and analysed by a computer. All creep experiments were conducted in a stress range between 10 and 60 MPa, at a temperature of 296 K, and at a creep duration which was constant and equal to 20 min. After unloading, the recovery of the strain was also studied for 1 h.

3. Results

All creep tests for every crystallinity ratio were carried out on the same sample in ascending order of stress so that the physical state of the material was not modified. The general shape of creep curves, $J(t)$, obtained for various values of the applied stress, σ, at a constant temperature will be described later. At low stress levels, the material behaved linearly and the strain was proportional to the stress (i.e. the creep compliance $J(t)$ was independent of stress). At higher stresses, $J(t)$ became dependent on the stress level. With increasing stress, the sample became easier and easier to deform.

To describe the role of stress on the creep behaviour, a particular value, σ_c, of the stress was used [7]; σ_c is defined as follows

$$\frac{J_{max}(\sigma_c) - J_{max}(0)}{J_{max}(0)} = 10\% \qquad (1)$$

where J_{max} is the creep compliance at the end of the creep time. Obviously, there is no critical stress. But below σ_c, there is no significant variation of the creep compliance curves with the stress compared to the experimental accuracy. Above σ_c, the separation of the creep curves becomes clearly apparent. Moreover, this value, σ_c, remains insensitive to change of creep duration [7].

Fig. 1 represents two creep curves obtained with the amorphous and semicrystalline films ($X_c = 41\%$). We notice that for the same conditions of temperature and stress, creep curves of the semicrystalline sample remain below those for the amorphous sample. Different values of σ_c, E, $E(t_c)$ are used to follow the evolution of the creep behaviour during annealing. E actually corresponds to the relaxed modulus for a stress near zero at 5 s after loading. $E(t_c)$ is the relaxed modulus at 1200 s, i.e. at the end of the creep time; in practice, it corresponds to the inverse of $J_{max}(0)$. These values are obtained with an accuracy of a few megapascal for σ_c and of about 10% for E and $E(t_c)$, which is enough to observe the effect of crystallinity. In order to compare the three variations versus crystallinity, the norm, N, is used. For instance, for a given crystallinity ratio X_c, N is defined by the function

$$N(X_c) = \frac{E(X_{c\,max}) - E(X_c)}{E(X_{c\,max}) - E(X_{c\to 0})}. \qquad (2)$$

Fig. 2 represents the variation of the norm of σ_c, E, $E(t_c)$ versus crystallinity. The three parameters follow the same tendency: they increase with the crystallinity following two sigmoidal curves: the first below a crystallinity of 36% corresponding to a T_c of 403 K, the second above 36%. These two variations can be explained by the morphological aspects of the crystallization. In fact, the crystallization process takes place in two stages [4]. At low temperatures ($T_c < 403$ K) the primary crystallization occurs. Part of the amorphous phase is transformed into crystalline lamellae. The first stage must be related to the increase of σ_c, E and $E(t_c)$ of about 50%. The second increase is due to the secondary crystallization process during which the crystallization develops further in the amorphous regions between the lamellae. This latter stage improves the three properties by about 50%. Pastor *et al.* [8] and Balta-Calleja *et al.* [9] found the

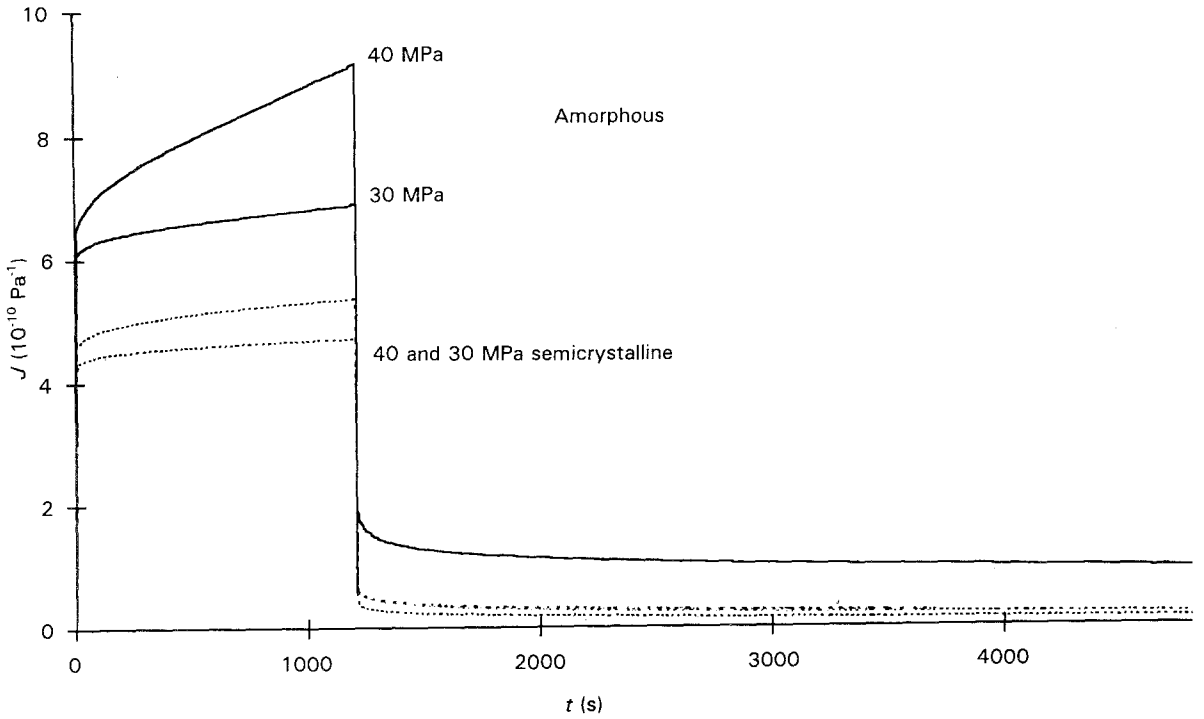

Figure 1 Influence of stress. Creep curves obtained on (——) amorphous and (– – –) semicrystallized of $X_c = 46\%$ PET for two stresses, 30 and 40 MPa.

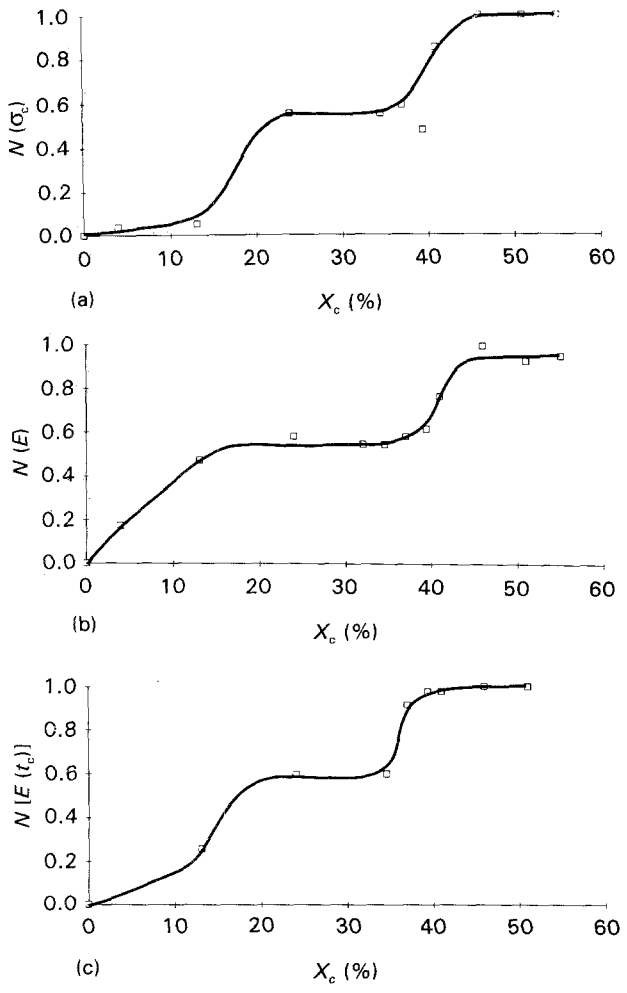

Figure 2 Variation of (a) σ_c, (b) E, (c) $E(t_c)$ with the crystallinity ratio. These variations are represented by the function $N(X_c)$, which is defined for a given crystallinity ratio X_c (see text).

same sigmoidal variations on annealed PET samples with microhardness measurements.

In conclusion, it can be stated that creep experiments again indicate the occurrence of two crystallization stages. The three values σ_c, E, $E(t_c)$, which are independently determined, confirm the existence of two sigmoidal curves. Thus the creep experiment is very sensitive to the morphological changes and creep appears to be an excellent practical tool by which to control the crystallization process.

4. Theoretical approach

The semicrystalline PET exhibits both amorphous and crystalline parts. The deformation of the amorphous region can be analysed as described below. The two-phase aspect accounts for the mechanical coupling between the two phases. For this purpose, a phenomenological mixing law will be introduced.

4.1. The amorphous phase

In order to analyse the mechanical behaviour of the amorphous part of PET in creep experiments [7], we used the molecular model developed in our laboratory [5, 10, 11], in which the microscopic behaviour is related to local molecular motions. This theory is based on the following assumptions. The amorphous polymer is considered to be a close packing of molecular units in which there are microregions corresponding to microfluctuations in the density, having an increment of enthalpy and entropy and called quasi point defects (QPD); it is possible to evaluate their concentration, C_d, by differential scanning calorimetry.

By thermomechanical activation, the QPD become activated, and sheared-microdomains (SMD) are nucleated. If the applied stress remains, SMDs expand owing to correlated molecular motions with a characteristic time equal to τ_{mol} (time for a translational motion of a structural unit over a distance comparable to its size).

$$\tau_{mol}(\sigma) = t_0\left[\frac{\tau_\beta(\sigma)}{t_0}\right]^{1/\chi} \quad (3)$$

where χ is a correlation parameter which depends on the defect concentration C_d, ($0 < \chi < 1$; $\chi = 0$: in the case of perfect crystal $C_d = 0$, $\chi = 1$: in the case of perfect gas, $C_d = 1$ ($\tau_{mol} = \tau_\beta$)), t_0 is a time scaling parameter. The time $\tau_\beta(\sigma)$ corresponds to the thermomechanical activation of an elementary molecular process; it is generally given by an Arrhenius equation of the form

$$\tau_\beta(\sigma) = \tau_0 \exp\left\{\frac{U_\beta[1 - \sigma/\sigma_0]^{3/2}}{kT}\right\} \quad (4)$$

with $\sigma_0 = G_0/2\pi$, G_0 the shear modulus at 0 K, U_β the thermal activation energy and τ_0 time which is proportional to the inverse of the Debye frequency.

For experimental times, shorter than τ_{mol}, the expansion of SMD occurs due to conformational changes. The elastic energy associated with SMD implies their reversible constriction after the removal of the stress. The SMD expansion leads mainly to the anelastic strain. Whereas for longer experimental times, there is annihilation of the lines bordering the SMD and loss of the elastic energy, this leads to an irreversible shear strain. These assumptions lead to the expression of the elastic, anelastic and viscoplastic components of the creep compliance

$$J(t) = J_u + A\left[1 - \exp\left\{-\left[\frac{t}{\tau_{mol}(\sigma)}\right]^{1/\chi_e}\right\}\right] + A'\left[\frac{t}{\tau_{mol}(\sigma)}\right]^{\chi'} \quad (5)$$

J_u corresponds to the unrelaxed compliance, A represents the anelastic equilibrium compliance and A' is proportional to the relaxation strength. χ_e corresponds to the average value of the correlation parameter material as a whole. χ' is another correlation parameter characterizing the ability of chain reorientation around the SMD when the times become long enough [10].

In fact, the distribution of relaxation times must be accounted for. Thus, a gaussian distribution function in the distribution factor of the correlation parameter $1/\chi_i$ between 1 and $1/\chi_e$ is used [5]. It results in a time distribution between τ_β and τ_{mol}.

Finally, the creep compliance is given by the following theoretical formulation:

$$J(t) = J_u + A\left\{\sum g_i\left(1 - \exp\left[-\frac{t}{\tau_{mol_i}(\sigma)}\right]\right)\right\}\Big/\sum g_i + A'\left[\frac{t}{\tau_{mol}(\sigma)}\right]^{\chi'} \quad (6)$$

with

$$\tau_{mol_i}(\sigma) = t_0\left[\frac{\tau_\beta(\sigma)}{t_0}\right]^{1/\chi_i} \quad (7)$$

g_i is the statistical weight of events with time τ_{mol_i}. [5].

In the approximation of the low viscoplastic component, A' is chosen as equal to A. This theory was applied to the amorphous part of the PET. The parameters τ_0, U_β and σ_0 are estimated from mechanical spectroscopy and are, respectively, equal to 1.7×10^{-16} s, 0.56 eV, 380 MPa. Moreover, $\chi' = 0.8$ and $t_0 = 10^{-11}$ s have been previously determined by Benatmane [6].

A and χ, which are material parameters, are determined by numerical calculation using Equation (6). These coefficients are adjusted so that the sum

$$S = \sum_{i=0}^{n} (J_{exp} - J_i(\chi_i, A_i))^2 \quad (8)$$

is minimized. J_{exp} and J_i are, respectively, the experimental data and the theoretical values. All the calculations are worked out with 100 discretization points. Thus the accuracy of the parameters A and χ corresponds to the step used for calculation. Typical values obtained with this method for amorphous PET are $\chi = 0.27$, and $A = 2 \times 10^{-10}$ Pa^{-1}. These values are in agreement with the data obtained by other experimental techniques such as differential scanning calorimetry or low-frequency mechanical spectroscopy [6]. There is quite a close correlation between the experimental creep curves and the predicted ones. There appears, however, to be a slight discrepancy at the beginning of the recovery in the non-linear domain. Attempts will be made to explain this later.

4.2. Semicrystalline PET

The two-phase nature of the semicrystalline PET enables us to use directly the molecular model of non-elastic deformation. The amorphous and crystalline phases present very different mechanical properties. The creep behaviour depends, to a great extent, on the mechanical coupling of the two phases. The behaviour of the amorphous phase is supposed to be described by the above theory. The crystalline part is considered as a perfect crystal which does not present anelasticity. Thus the crystalline compliance is defined by $J_u(t) = 1/E_c$. The elastic modulus of the perfect crystal of PET has been determined [12] by theoretical approaches. The E_c value has been estimated to be in the range 100–130 GPa for the main direction and at 6 GPa in a perpendicular direction. These values have been determined in the direction parallel and perpendicular to the chain axis. In our case, crystallization is obtained by thermal treatments on isotropic amorphous samples. Thus in this work, the average value of 20 GPa is retained. Nevertheless, a difference in E_c value does not really affect the conclusions.

To take into account the two-phase structure of the semicrystalline films, it is necessary to introduce a coupling law, to describe the mechanical behaviour of the material as a whole. A great deal more needs to be known about this aspect of the two-phase material

but, in fact, the only established laws are the two well-known Reuss and Voigt limits, corresponding to the additivity of strain and stress, respectively. Various approaches have been proposed to find the right position between these two limits, but most of them introduce an adjustable parameter. A series parallel model, previously used by Takayanagi *et al.* [13] will be used to express the coupling effects (see Fig. 3). This model leads to the following expression giving the creep compliance, J_{sc}, of the whole material as a function of the amorphous and crystalline compliances, J_a and J_c

$$\frac{1}{J_{sc}} = \frac{1-\phi}{J_a} + \frac{\phi}{J_c + (1-\lambda)J_a} \quad (9)$$

This formulation implies two parameters, λ and ϕ, linked by the equations: $V_c = \lambda\phi$ and $V_{as} = (1-\lambda)\phi$, where V_c and V_{as} correspond, respectively, to the volume fraction of the crystalline and the amorphous series phases. In such a model, λ is considered as an adjustable parameter. However, using the work of Fulchiron *et al.* [14], who have related the parameter λ to the amorphous volume fraction, we ensure the description of the mechanical coupling without adjustable parameter. They have supposed that this amorphous volume fraction, V_{as}, is proportional to the reciprocal long period. In the crystallization temperature range studied in this work, this long period evolves only slightly (between about 9 and 11 nm). Thus, they considered that the crystalline surface remains quasi unchanged. Following the assumption that the coupling is dependent on the available surface, S_c, of the crystalline lamellae, they considered that if S_c is constant, the amorphous fraction, V_{as}, ensures the coupling remains constant. Thus λ is calculated from the expression

$$\lambda = \left[\frac{V_{as}}{V_c} + 1\right]^{-1} \quad (10)$$

V_{as} is estimated by tensile modulus measurements to be $V_{as} = 0.2$.

Finally, the creep compliance of the semicrystalline PET is given by

$$J_{sc} = \frac{J_a[\lambda J_c + (1-\lambda)J_a]}{\lambda J_c + (1-\lambda)J_a + V_c(J_a - J_c)} \quad (11)$$

λ is calculated from Equation 10, using the assumption that V_{as} remains constant. This is not true at the beginning of the crystallization ($X_c < 33\%$) because of the three-dimensional growth of the crystallites: in that case, the surface of the lamellae does not remain constant. This is why this model will only be used for crystallinity ratios higher than 29%.

The amorphous creep compliance, J_a, is deduced from the molecular model with the same values U_β, τ_0 and t_0, because crystallization does not affect the β relaxation process [14, 15]. χ' is estimated to be lower than for the bulk amorphous PET ($\chi' = 0.6$); in effect, the crystallization acts as a physical cross-linking. χ and A are always determined as previously explained.

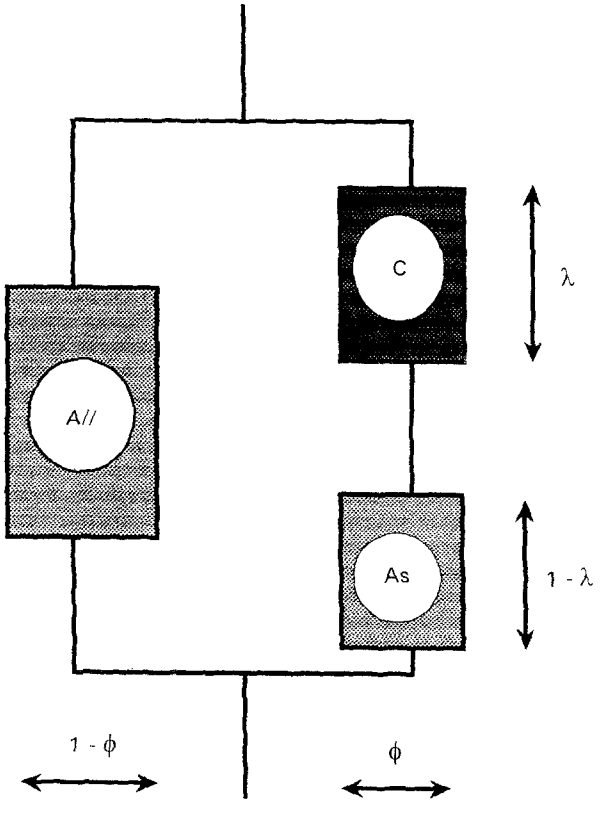

Figure 3 Representation of the series parallel model.

4.3. Discussion

In Table I, the variation of A and χ with the stress is displayed for all crystallinity ratios. The following comments can be made.

(i) A is higher for the amorphous part of the semicrystalline PET than for the bulk amorphous (5.5×10^{-10} Pa^{-1} compared to 2×10^{-10} Pa^{-1}).

(ii) A is not sensitive to the crystallinity ratio.

(iii) A is stress dependent in the non-linear domain (5.5×10^{-10} Pa^{-1} for low stresses and 8×10^{-10} Pa^{-1} for a stress of 60 MPa in the case of 41% crystallized sample).

(iv) The correlation parameter, χ, is slightly lower for the amorphous part of the semicrystalline sample than for the bulk amorphous (0.23 compared to 0.27).

(v) χ is slightly influenced by the stress for almost all the semicrystalline samples (0.24 for low stress against 0.22 at high stress).

An approach developed on a physical basis is required to explain these results.

(i) Owing to the physical meaning of A, its increase with the crystallization indicates that the defect concentration in bulk amorphous polymer is lower than in the amorphous part of the semicrystalline one. A direct approach could explain the increase in defect concentration introduced by annealing. With infrared spectroscopy measurements, Lin and Koenig [3, 16] studied the chain conformation changes of PET submitted to annealing. Two different conformations are present: the "gauche isomer" corresponding to a defect conformation, which exists only in the amorphous phase, and the "trans isomer" which is present in both phases. Before any thermal treatments, Lin and Koenig observed 13% trans conformations and 87%

TABLE I Variation of the creep equilibrium compliance and correlation parameter with the stress and the crystallinity ratio

Stress (MPa)	X_c(%)													
	0		29		34		37		39.5		41		46	
	A	χ	A	χ	A	χ	A	χ	A	χ	A	χ	A	χ
20	2	0.27	5.5	0.23	5.5	0.24	5.5	0.23	5.5	0.23	–	–	5.5	0.24
25	2	0.27	5.5	0.23	5.5	0.24	5.5	0.23	5.5	0.23	–	–	5.5	0.24
30	2	0.27	5.5	0.225	5.5	0.235	5.5	0.23	5.5	0.23	5.5	0.24	5.5	0.235
35	2	0.27	5.5	0.22	5.5	0.235	5.5	0.23	5.5	0.23	5.5	0.23	5.5	0.23
40	2.3	0.27	–	–	5.5	0.23	6	0.225	5.5	0.23	6	0.335	5.5	0.23
45	–	–	–	–	6	0.23	6.5	0.22	6.5	0.227	6.5	0.22	5.5	0.225
50	–	–	–	–	7	0.225	7	0.22	7	0.22	7	0.22	5.5	0.22
55	–	–	–	–	8	0.225	–	–	–	–	7.5	0.22	6	0.217
60	–	–	–	–	–	–	–	–	–	–	8	0.217	6.3	0.214

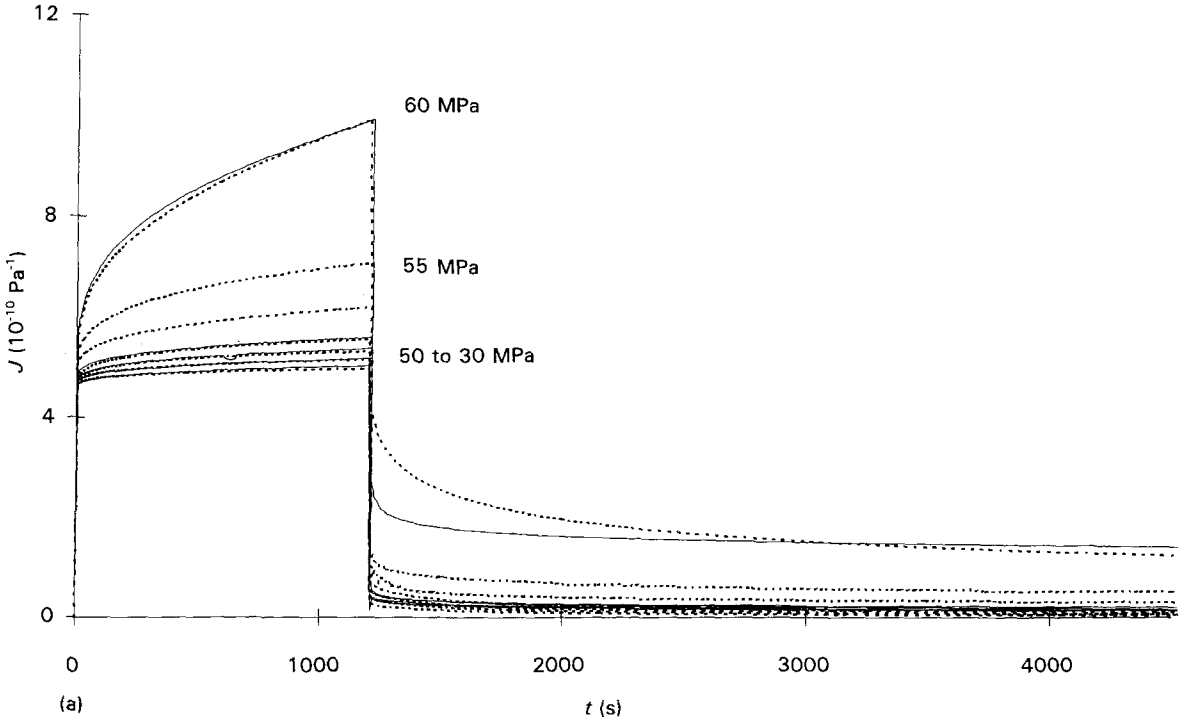

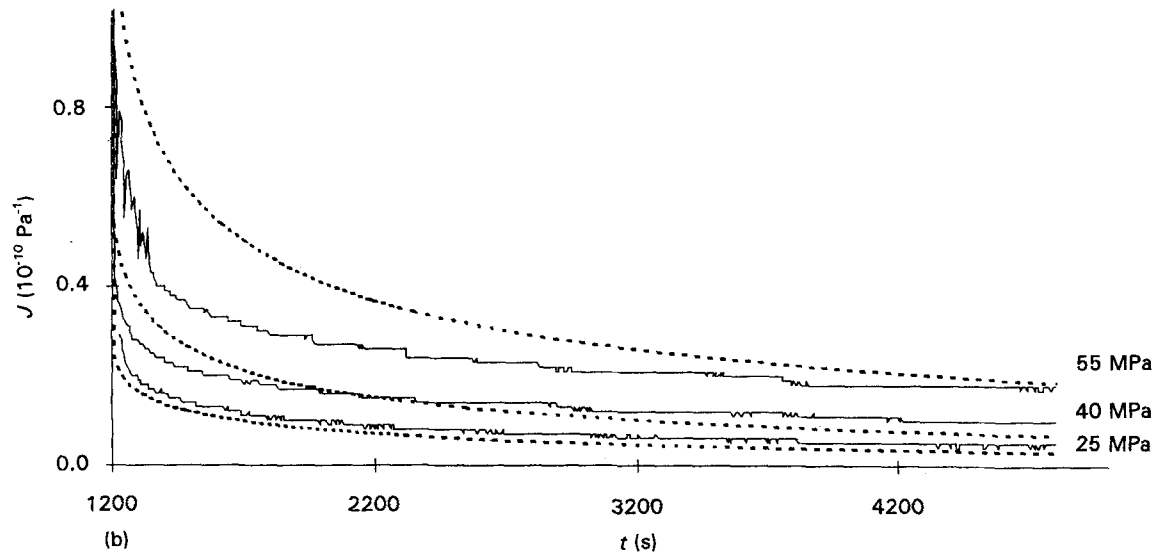

Figure 4 (a) Creep curves obtained by testing (——), compared to the prediction (– – –), in the case of a semicrystalline sample (X_c = 41%). When the prediction and experiment are superimposed for a given stress, only the theoretical curve is represented (- - -). (b) Enlargement of (a), but only for the recovery.

"gauche" in the wholly glassy polymer. When crystallization occurs, the gauche–trans isomerization leads to a rapid decrease in trans amorphous contents which nearly falls to zero. Lin and Koenig have associated these trans conformations with the extruded chain units making up the interlamellar links. Thus, the loss of the trans amorphous content must correspond to a decrease in the number of tie molecules, consequently, a loss in tenacity should be expected. If we assume that gauche conformations are the less ordered (compared to the trans conformations), their concentration can be assimilated to that of the quasi point defects. So, the fall in trans amorphous content is in agreement with the increase of the parameter A, which corresponds to the defect concentration.

(ii) The trans content diminution occurs very rapidly during the first stage of crystallization and remains nearly at zero for the second step of crystallization. The range of crystallinity ratios we have studied, corresponds mostly to this second stage, thus the decrease in trans isomer was insufficient to involve a change in A.

(iii) For this point, an energy profile representing the nucleation and growth of a sheared microdomain will be discussed in the next part of this work.

(iv) In annealed PET, the crystalline lamellae reduce the chain mobility of the amorphous phase. So the molecular motions should be more constrained. This effect is expressed in the decrease in χ with increasing crystallinity ratio [17].

(v) In the non-linear domain, where plasticity appears, all the strain is supposed to be localized in the amorphous domains, involving local molecular orientations. Indeed, for high stresses, the molecular stretching increases the correlation effects, so χ decreases.

Finally, all the experimental observations agree with the physical aspect of the molecular model. It is surprising that all the morphological changes induced during the two steps of the crystallization process involve sensitive changes in the physical parameters.

In order to understand the creep behaviour of semicrystalline PET, in the non-linear domain, we can analyse the curves obtained by experiments and by theoretical predictions. Theoretical curves are plotted in Fig. 4a, using Equation 6 for the amorphous part and Equation 9 for the mechanical coupling with the same set of parameters as previously described. The theoretical curves (dashed lines) are compared to the experimental one (full line). At first sight, the theory leads to a quantitative description of the experimental creep behaviour with both curves exhibiting the same general shape during creep. At low and medium stresses, the curves are superimposed. Accordingly, the σ_c value, previously defined and deduced from theoretical curves, follows the same variation as the experimental curves within an accuracy of 10%. However, for high stresses, even if the behaviour during load remains exactly the same for the experiment and prediction, a discrepancy appears in the rate of recovery (Fig. 4b). More exactly, for stresses higher than σ_c, during the early stages of the recovery, the recovered strain is always greater than that predicted. As recovery progresses, the difference between the two compliance curves becomes smaller. The observed residual compliance conforms fairly closely to the prediction. Furthermore, the more the stress increases in the non-linear domain, the later the two curves meet. Whatever the model used may be, the same discrepancy appears in the recovery between the prediction and the experiment [18, 19].

In order to explain those features, a scheme showing an energy profile will be used [20]. This energy profile shows the energy state of a microregion where a sheared microdomain is nucleated and expands. The line bordering an SMD is a Somigliana dislocation which cannot glide. Its elastic energy corresponds to $2\pi R(Gb^2/4\pi)\ln[(2/3^{1/2}b)R]$ with b the shear vector, G the shear modulus, and R the radius of an SMD. Applying a stress results in lowering the energy level because of the work done by the applied stress: $\pi R^2\sigma b$. In addition, to take into account the fact that SMD growth occurs, thanks to conformational changes with a local energy U_β, a succession of barriers are added. For a critical size of the SMD, the profile shows a lowering of the barriers, because the SMDs coalesce and dislocation energy is suppressed. Finally, a semi-quantitative reproduction is given in

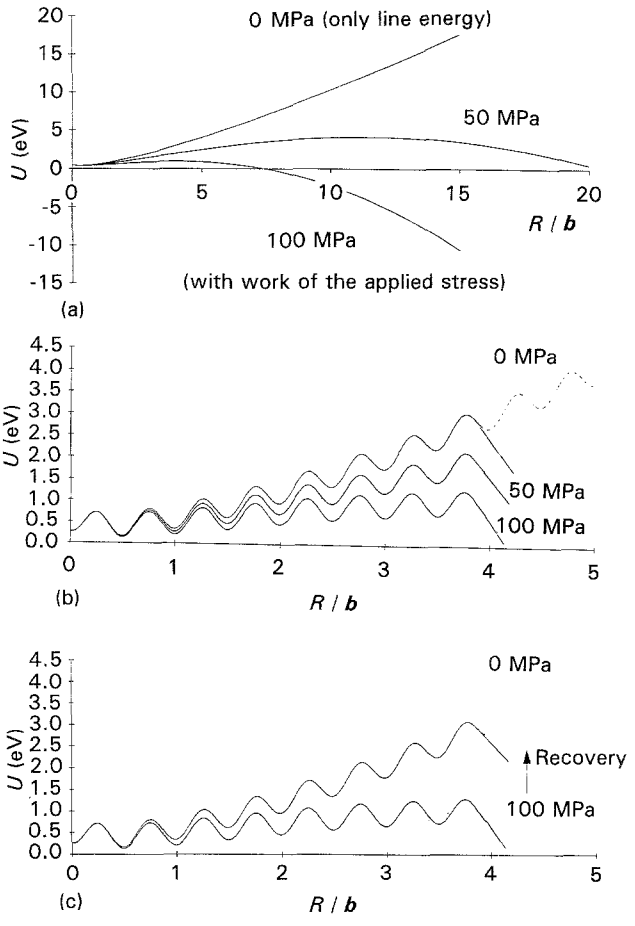

Figure 5 (a) Energy of a SMD versus its radius and variation when the profile is lowered because of the work of the applied stress. (b) As (a), but with (i) limitation of line energy due to SMD coalescence and (ii) barriers for conformational changes; the probable repartition of the population is modified. (c) The stress is removed, the recovery occurs, and the activated defects return to their initial state.

Fig. 5. Without any applied stress (Fig. 5a, for $\sigma = 0$ MPa), the energy state of an unactivated defect is mainly localized in the first well. The equilibrium population is calculated with the help of the Boltzmann statistic. When stress is applied, the whole profile is lowered by the stress field (Fig. 5b); there is a new equilibrium distribution of the defects in the several wells. Furthermore, this equilibrium changes with stress. This involves a non-linear increase in the equilibrium population with stress, which is expressed by the increase in the parameter A.

When stress is removed (Fig. 5c), the elastic energy stored during the SMD expansion causes the sheared regions to return to their unstressed initial states. From the energy point of view, the profile returns to its original state, but the energy barriers are lower than for the growth of an SMD. Thus by using this scheme, the high rate of recovery is easy to understand. Introducing this profile in the molecular model mentioned above should improve the description of the recovery and should give a better prediction of the non-linear behaviour.

5. Conclusion

A study of amorphous and crystallized PET has been carried out using creep experiments in the linear and non-linear domains. Analysis of creep compliance curves has shown that (i) for a given strain rate, creep strength increases with the crystallinity ratio, (ii) creep is sensitive to the morphological changes occurring during annealing.

The use of the molecular model of Perez [5] for the prediction of creep behaviour has given a quantitative description of experimental curves obtained in linear and non-linear domains. Indeed, the particular value of the stress σ_c, used to characterize the non-linear domain, is determined by the theory with an accuracy which is better than 10%. On the other hand, the model gives a good description of the recovery, even for medium stresses. For high stresses the theory does not reproduce correctly the beginning of the recovery. In that case, the use of the energy profile related to SMD nucleation could qualitatively account for the discrepancy.

To take into account the two-phase structure of PET, the mechanical coupling of crystalline and amorphous phases was supposed to follow a phenomenological series parallel model, in which the adjustable parameter is related to morphological considerations. This approach allowed us to understand the stress effects in the amorphous phase, for instance, the decrease in molecular mobility due to molecular stretching and the increase in the anelastic equilibrium compliance with stress.

References

1. A. SIEGMANN and E. TURI, *J. Macromol. Sci. Phys.* **4** (1974) 689.
2. G. GROENINCKX, H. REYNAERS, H. BERGHMANS and G. SMETS, *J. Polym. Sci.* **18** (1980) 1311.
3. SHAOW-BURN LIN and JACK L. KOENIG, *J. Polym. Sci.* **21** (1983) 2365.
4. G. VIGIER, J. TATIBOUET, A. BENATMANE, R. VASSOILLE, *Colloid Polym. Sci.* **270** (1992) 1182.
5. J. PEREZ, "Physique et mecanique des polymères amorphes" (Lavoisier, Paris, Technique et Documentation, 1992) p. 384.
6. A. BENATMANE, Thesis, Lyon (1991).
7. F. BOUQUEREL, P. BOURGIN and J. PEREZ, *Polymer* **33** (1992) 516.
8. J. M. PASTOR, A. GONZALEZ and J. A. DE SAJA, *J. Appl. Polym. Sci.* **38** (1989) 2283.
9. F. J. BALTA CALLEJA, C. SANTA CRUZ and T. ASANO, *J. Polym. Sci. B* **31** (1993) 537.
10. J. PEREZ and J. Y. CAVAILLE, *Trends Polym. Sci.* **2** (1991) 63.
11. J. Y. CAVAILLE and J. PEREZ, *Makromol. Chem. Makromol. Symp.* **35/36** (1990) 405.
12. K. NAKAMAE, T. NISHINO, Y. SHIMIZU and T. MATSUMOTO, *Polym. J.* **19** (1987) 451.
13. M. TAKAYANAGI, K. IMADA and T. KAJUAMA, *J. Polym. Sci.* **15** (1966) 263.
14. R. FULCHIRON, C. GAUTHIER and G. VIGIER, *Acta Polym.* **44** (1993) 313.
15. K. H. ILLERS and H. BREUER, *J. Colloid Sci.* **18** (1963) 1.
16. SHAOW-BURN LIN and J. L. KOENIG, *J. Polym. Sci.* **20** (1982) 2277.
17. G. VIGIER and J. TATIBOUET, *Polym.* **34** (1993) 4257.
18. R. N. HAWARD, "The Physics of Glassy Polymers" (Applied Science, London, 1973) p. 620.
19. P. DANG, Thesis, Poitiers (1991).
20. R. QUINSON and J. PEREZ, *Polym.*, submitted.

Received 2 August 1993
and accepted 13 April 1994